Planar-type tunnel junctions with $Bi_2Sr_2CaCu_2O_{8+\delta}$ high-temperature superconducting electrodes and $Bi_2Sr_2YCu_2O_{8+\delta}$ artificial barriers

E. Baca,[a] M. Chacón, W. Lopera, M. E. Gómez, and P. Prieto
Departamento de Física, Universidad del Valle, A. A. 25360, Cali, Colombia

J. Heiras
Instituto de Investigaciones en Materiales–UNAM, A. P. 70360, Mexico

R. Di Leo, P. Romano, and A. M. Cucolo
Unità INFM–Dipartimento di Fisica, Università di Salerno, I-84081 Baronissi, Italy

(Received 17 December 1997; accepted for publication 8 May 1998)

We performed a detailed study of the structure and transport properties of Bi2212/22Y2/2212 planar-type tunnel junctions. Both high-temperature superconducting electrodes and semiconducting barriers are highly epitaxial thin films deposited onto $SrTiO_3$ single-crystal (001) substrates. Deposition of the films was carried out by a high oxygen pressure dc-sputtering technique, which produces high-quality epitaxial thin films, as determined by x-ray diffraction, lattice resolution transmission electron microscopy, and Rutherford backscattering. Critical temperatures for the superconducting electrodes of 85 K were determined by transport measurements (ρ and χ versus T). A study of resistivity as a function of temperature of the semiconducting barriers was performed. Clear quasiparticle tunneling indicating a gap structure at about 30–35 mV, a zero-bias peak, as well as linear and flat background at high voltages have been observed. For junctions with very thin barriers weak-link-type behavior was observed. An analysis of the $I-V$ curves for these junctions has been made based on the resistively shunted junction model. © *1998 American Institute of Physics.* [S0021-8979(98)00516-7]

I. INTRODUCTION

There are many reasons to expect that planar-type heterostructures, involving high-temperature superconducting thin films will have important applications in microelectronics,[1,2] cybernetics,[3] and other fields. In fact, several devices based on high-temperature superconductors (HTS) have already been developed, particularly those involving superconducting quantum interference devices (SQUIDs).[4] However, it is also well known that HTS are difficult materials to handle: they are fragile metal oxides prepared at high temperatures. From a pure scientific point of view, HTS are ceramic materials with fairly complicated composition and structure; and furthermore, the mechanisms that lead to superconductivity in these materials are essentially unknown.

HTS are the subject of many research efforts throughout the world. These HTS belong to three compound families: cuprates, bismuthates, and fullerites, where the cuprates have superconducting transition temperatures ranging from a few kelvin to 134 K in $HgBa_2Ca_2Cu_3O_{8+\delta}$ at ambient pressure and 164 K at high pressure (30 GPa).[5] Some of them, such as those based on Y, Bi, and Tl, have a basic composition and variations of the latter gives rise to different superconductors within a family.[5] YBCO, the first superconductor reported with a T_C higher than 77 K, is being widely studied in many laboratories. Two other superconducting families, considered important from the applications point of view, are those based on Bi and Tl. Of these, the latter has a member with a T_C as high as 130 K at high pressure; however, it has the problem of being highly toxic. The other family, the one based on Bi, is interesting in spite of having lower T_C's, since it is not as toxic as the Tl family. At present, there are three recognized superconducting phases within the Bi-22$(n-1)n$ system[5] with $n=1$ (2201), 2 (2212), and 3 (2223), showing the layered stacking sequence of $(BiO)_2(SrO)(CuO_2)(Ca)$ $(CuO_2)\cdots(Ca)$ (CuO_2) (SrO) with $n(CuO_2)$ layers separated by $n-1$ Ca layers with some interesting structural modulations in the $(BiO)_2$ layer.[5] They have similar layered structures and are chemically stable. This is one reason to consider BSCCO as a good candidate for device development.

Since 1960, tunneling spectroscopy has become established[6] as a powerful technique to investigate superconductors. The differential tunneling conductance versus voltage of a tunnel junction is directly related to the density of states and provides accurate measurements of the energy gap and the electron–phonon coupling in conventional superconductors. There are no fundamental reasons why tunneling cannot provide similar information for HTS. Several tunneling techniques have been applied for understanding of HTS: break junctions,[7–9] point-contact junctions,[10–12] grain-boundary junctions,[13] squeezable junctions,[14] scanning tunneling microscope vacuum junctions,[15] step-edge junctions,[16] and planar junctions.[17–19] In all cases the interface should be very clean, with the composition and structure homogeneous and very sharp (within one coherence length, which may be extremely small for HTS) since tunneling is very sensitive to

[a]Electronic mail: bacca@calima.univalle.edu.co

surface properties. Therefore, producing a good tunnel junction with HTS electrodes is a formidable challenge to experimentalists.

Several devices are based on planar heterostructures, i.e., multiple planar layers involving HTS and other nonsuperconducting materials. Planar-type heterostructures are important since their method of production is compatible with the one used to produce semiconducting devices and, therefore, they may be incorporated in the production of superconducting/semiconducting mixed devices in a natural way. These devices may be produced from sandwich-type structures where there are two electrodes separated by an intermediate layer that usually is not a good conductor; there are several types of planar junctions which, depending on the nature of the electrodes and intermediate materials, are called SIS (superconductor/insulator/superconductor), SNS (N stands for normal, as opposed to superconducting material), S/S*/S (S* stands for semiconductor), SIN (superconductor/insulator/normal), etc. These sandwich-type tunnel junctions are very important, not only because they are natural precursor to SQUIDs and other similar practical devices, but also because tunneling, as mentioned before, may provide information about the superconducting properties of the electrodes which form the junctions.[20]

Heterostructures and other types of junctions based on YBCO have been also studied,[21,22] whereas only a few studies have been carried out on junctions based on BSCCO.[23,24] The key for producing good tunnel junctions is the nature and quality of the intermediate layer, and particularly, the quality of the interfaces which are formed with the electrode materials. An ideal barrier material will be one that, apart from being a good insulator and pinhole free, has a close matching of lattice parameters and similar composition to the HTS electrode to be investigated. The first condition is necessary for a stress-free epitaxial growth of the top electrode and sharpness of both interfaces. The second condition is necessary to assure that foreign atoms may not interdiffuse through the interface and degrade the surface of the superconducting electrodes. It is also desirable that the barrier has a similar thermal expansion coefficient. With this in mind, Mizuno *et al.*[23] have reported studies on planar-type SNS junctions of $Bi_2Sr_2CaCu_2O_{8+\delta}/Bi_2Sr_2CuO_{8+\delta}$ (or $Bi_2Sr_2NdCu_2O_x/Bi_2Sr_2CaCu_2O_{8+\delta}$ employing the Ca deficient phase, 2201, or $Bi_2Sr_2NdCu_2O_x$ as barrier materials obtaining Josephson weak-link-like behavior, and Cucolo *et al.*[24] have reported quasiparticle tunneling in planar $Bi_2Sr_2CaCu_2O_{8+\delta}/Bi_2Sr_2YCu_2O_{8+\delta}/Bi_2Sr_2CaCu_2O_{8+\delta}$ heterostructures using $Bi_2Sr_2CaCu_2O_{8+\delta}$ (22Y2) as a barrier. The substitution of Ca^{2+} by Y^{+3} in the BSCCO 2212 phase leads to a $Bi_2Sr_2YCu_2O_{8-\delta}$ semiconductor, without drastic changes in the original structure[25,26] but with the additional advantage of high resistance at low temperatures, as will be seen. It is, in principle, a good barrier material to test in conjunction with BSCCO electrodes: both exhibit the same structure with a close lattice match and almost the same composition.

We have produced heterostructures involving HTS electrodes of $Bi_2Sr_2CaCu_2O_{8+\delta}$ with intermediate layers of $Bi_2Sr_2YCu_2O_{8+\delta}$ starting from thin films of very high quality in composition, structure, and texture. The obtained tunneling barrier is clean, has fairly sharp interfaces, and is pinhole free. In this article we report the method of production, characterization, and electrical properties of heterostructures of the type $Bi_2Sr_2CaCu_2O_{8+\delta}/Bi_2Sr_2CuO_{8+\delta}/Bi_2Sr_2CaCu_2O_{8+\delta}$, which are precursors to well-behaved SQUIDs and other practical devices.

II. EXPERIMENT

Superconducting, 2212, and semiconducting, 22Y2, thin films were deposited *in situ* using a high-pressure dc-sputtering process. Details of this technique have been previously described.[24,27] Therefore, only a short description will be given. Stoichiometric sintered $Bi_2Sr_2CaCu_2O_{8+\delta}$ and $Bi_2Sr_2YCu_2O_{8+\delta}$ sputtering targets of 35 mm diam and 10 $\times 10$ mm^2 substrates of single-crystal (001) $SrTiO_3$ were utilized. Pure oxygen at a pressure of 4.0 mbar was used as sputtering gas; this relatively high pressure avoids etching of the films by negatively charged oxygen ions. The substrate temperature was held constant during deposition close to 780 °C; after deposition, the films were annealed during 45 min at the same pressure and temperature; further annealing for 30 min at 600 °C in high vacuum was performed; finally, the films were cooled down to room temperature in the deposition chamber. Deposition rates were approximately 100 nm/h for all films; film thicknesses were controlled by measuring the deposition time at a constant sputtering rate. This deposition procedure consistently produces *c*-oriented epitaxial 2212 and 22Y2 thin films with smooth and very flat surfaces as probed by several analytical techniques (see below).

The 2212/22Y2/2212 trilayers were prepared by sequential sputtering of the films, each of them under similar conditions. The thickness of the films was approximately 200 nm for the electrode films while the barrier thickness varied between 8 and 12 nm. X-ray analysis of the films show exclusively $(0,0,2l)$ peaks, indicating the absence of foreign phases and a strong *c*-axis orientation of the films as shown in Fig. 1(a). Careful measurements of the rocking curve in the (0010) peak show a full width at half maximum (FWHM) of 0.28°. This low value supports the idea that the films are highly textured [see the inset of Fig. 1(a)].

Interface microstructure and quality were determined by cross-sectional lattice resolution transmission electron microscopy (TEM) using a Jeol 4000 EX electron microscope. It was observed that interfaces were very sharp and clean with no interdiffusion between layers; the intermediate film was pinhole free. A typical image is shown in Fig. 1(b).

Rutherford backscattering (RBS) and channeling measurements with 2.0 MeV/He ions were carried out in order to examine the composition and crystalline quality of the layers. RBS spectra for the 22Y2 layer, and for the complete trilayer 2212/22Y2/2212 are shown in Fig. 2. Comparison of the random spectrum with a computer simulation[26] gives film thickness and stoichiometry that correspond roughly to $Bi_2Sr_2CaCu_2O_{8-\delta}$ with a small deficiency in the Cu content. Since the back edges of the contribution to the spectrum from the different elements are quite steep, it is concluded

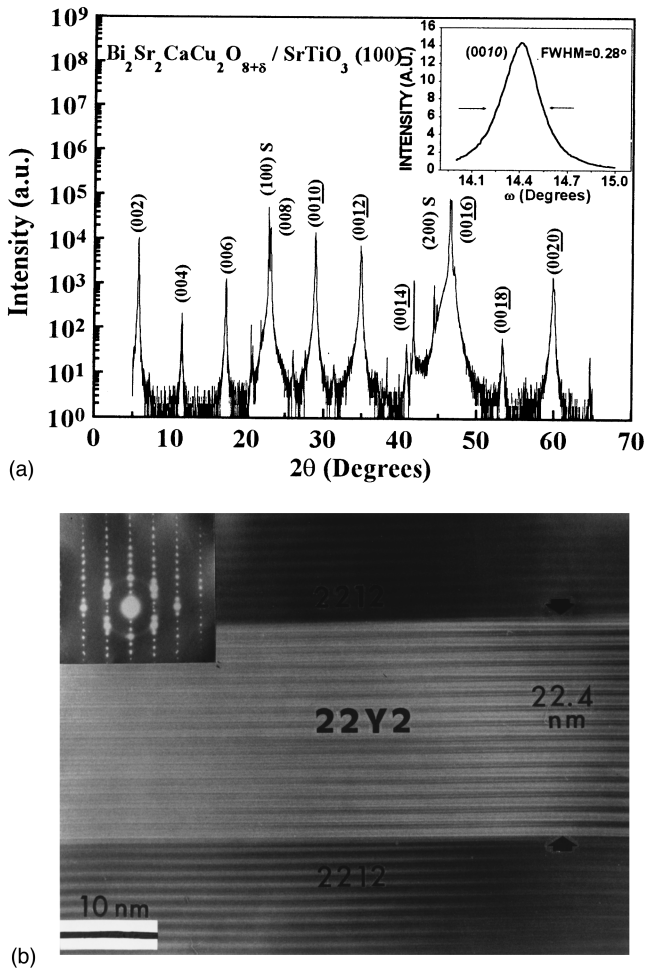

FIG. 1. (a) X-ray diffraction pattern of a 2212 film on a $SrTiO_3$ (001) substrate. Notice that only (002*l*) peaks appear; the inset shows the rocking curve with a small FWHM. (b) High-resolution TEM cross-section micrograph of a $Bi_2Sr_2CaCu_2O_{8-\delta}/Bi_2Sr_2YCu_2O_{8-\delta}/Bi_2Sr_2CaCu_2O_{8-\delta}$ trilayer showing the interfaces between the superconducting 2212 films and the 22Y2 barrier. The inset shows the selected-area diffraction pattern at an interface.

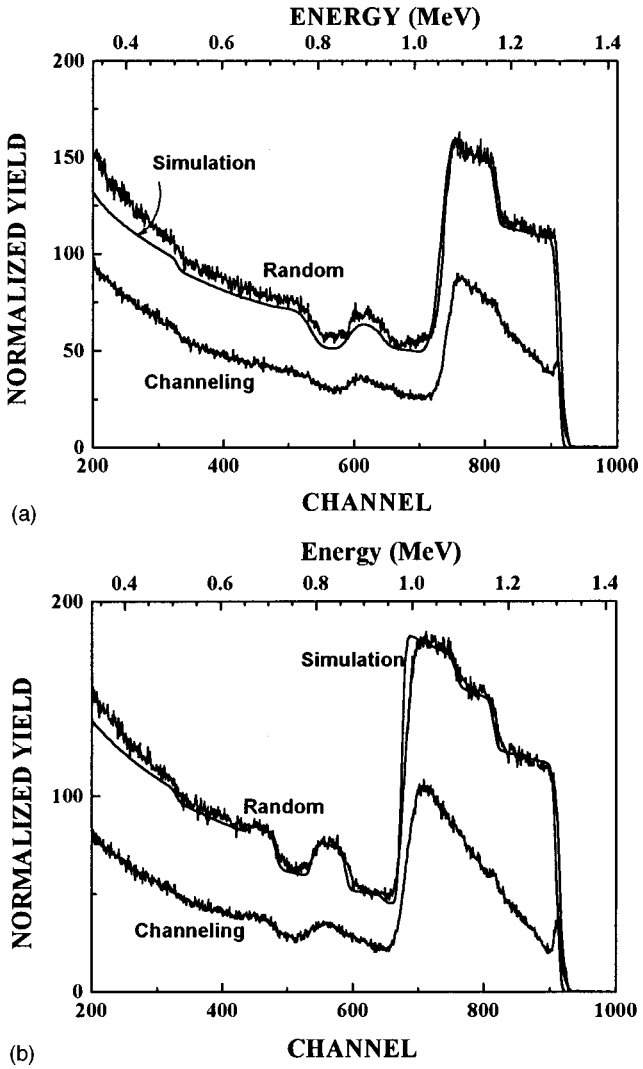

FIG. 2. RBS spectrum under random incidence and channeling conditions for the (a) $Bi_2Sr_2YCu_2O_{8-\delta}$ film and (b) $Bi_2Sr_2CaCu_2O_{8-\delta}/Bi_2Sr_2YCu_2O_{8-\delta}/Bi_2Sr_2CaCu_2O_{8-\delta}$ trilayer.

that the interfaces are fairly sharp, that is, no smearing from interdiffusion is observed. Alignment of the substrate such that the direction of the incident He beam is perpendicular to the surface results in a strong reduction of the backscattering yields for the single layers and a small reduction in the case of the trilayer; in particular, the ratio of the aligned signal to the random spectrum for Bi is about 40% near the surface region, further supporting the epitaxial quality of the films.

For tunneling measurements the trilayers were structured in cross-type junctions as shown in the Fig. 3. Patterning was made photolithographically by wet chemical etching, with diluted hydrochloric acid, from which 100 μm strips and 100×100 μm^2 junctions were obtained. The transition temperatures of the 2212 superconducting films were not affected by the patterning process, as shown in Fig. 4(a). Resistivity measurements were made on strips and tunneling on cross-type junctions, whereas ac-magnetic susceptibility measurements were also carried out on the trilayers by using the standard inductive method. Standard four-probe resistivity measurements were performed on all films. The superconducting transition temperature of both electrodes and the trilayer was obtained at ~85 K.

Resistivity measurements of a typical 22Y2 film is shown in Fig. 4(b); a semiconductorlike temperature dependence is clearly apparent in Fig. 4(b). Notice that it has a resistivity of about 50 $\mu\Omega$ cm at room temperature; this value is only two orders of magnitude higher than 2212 films

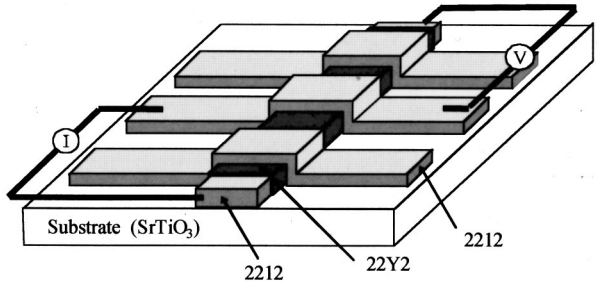

FIG. 3. Geometry of the trilayer structures after of the photolithography process.

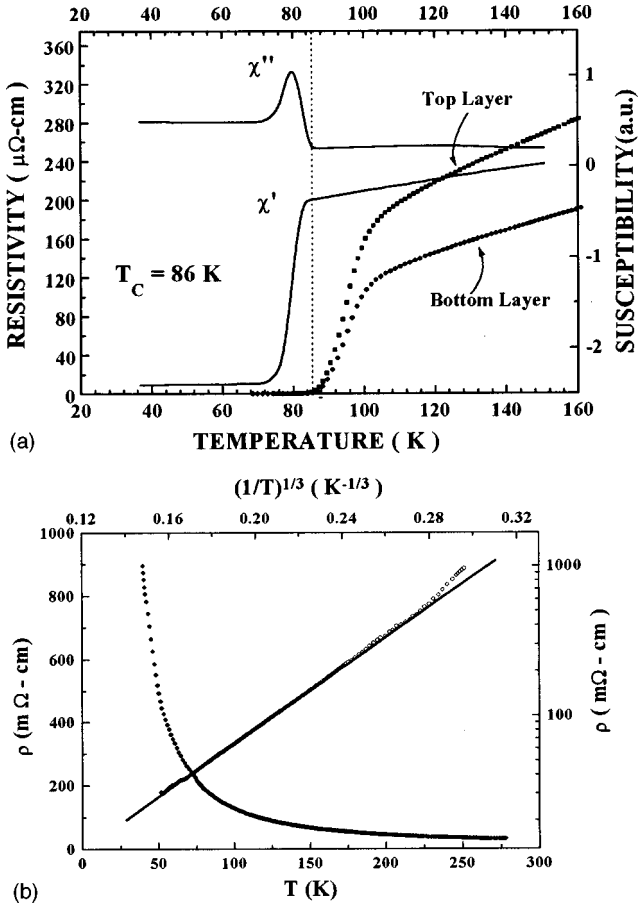

FIG. 4. (a) Resistivity as a function of temperature for bottom and top 2212 strips for a typical $Bi_2Sr_2CaCu_2O_{8-\delta}/Bi_2Sr_2YCu_2O_{8-\delta}/Bi_2Sr_2CaCu_2O_{8-\delta}$/trilayer structure after the photolithography process was completed; and ac-magnetic susceptibility as function of the temperature of the trilayers without the etching process. (b) Resistivity as a function of temperature for the 22Y2 barrier layer; plot of ρ vs $T^{-1/3}$, from which fit α and k_BT_0 are extracted.

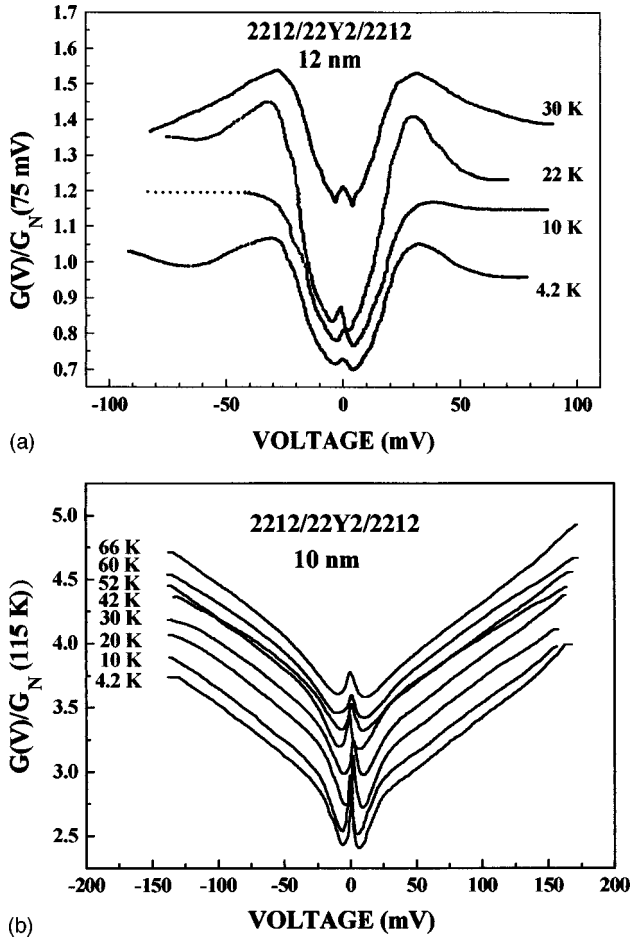

FIG. 5. Tunneling conductance vs voltage for the trilayer at different temperatures: (a) with flat background and (b) linearly increasing background. Curves have been displaced arbitrarily for clarity.

but increases drastically at low temperatures as shown in Fig. 4(b), and behaves almost as an insulator with clear advantages over other materials. This behavior cannot be described by thermally activated conduction given by $\rho \propto \exp(1/T)$. One can fit[28] $\rho=\rho_0 \exp(T_0/T)^{\alpha}$ to the experimental ρ versus T in order to investigate the possible electronic transport mechanism in 22Y2; here, T_0 is a characteristic temperature related to the decay length for the wave function of the localized states, while the α parameter can be written as $\alpha=(n+1)/(n+D+1)$, where D is the dimensionality of the hopping process and n describes the energy dependence of the density-of-state $N(E)$ near the Fermi level. If $N(E)$ is a constant then $\alpha=1/3$ for $D=2$. The inset of Fig. 3(b) shows a fit of ρ versus T from which the parameters α and T_0 are obtained. Notice that a good fit is obtained in the linear region from 40 to 260 K for the following values of $\alpha=0.33$ and $kT_0=19$ meV, indicating a bidimensional process and showing that hopping between localized states within the energy gap is the probable mechanism of conduction in 22Y2.

III. TUNNELING MEASUREMENTS

A. Quasiparticle tunneling

Quasiparticle tunneling characteristics were obtained via usual modulation techniques.[20] The differential tunneling conductance $G=dI/dV$ versus V was measured at different temperatures from 4.2 to 150 K at modulation voltages from 0.3 to 5 mV (always lower than thermal smearing), as is shown in Figs. 5(a) and 5(b). The $G(V)$ measurements of all junctions can be divided into three voltage ranges. In the *background range* for voltages higher than a certain gap voltage V_g, the $G(V)$ curves show a linear or flat background. In the *intermediate range* at voltages smaller than V_g and larger than about 5 mV a conductance decreasing could be seen with decreasing of the temperature due to the opening of a superconducting gap. The *low-voltage range*, $|V|<5$ mV was characterized by a zero-bias conductance peak, with its size depending on the temperature. Each range provides information about very different physical transport properties in the interface and superconducting electrodes.

In the *background range, linear behavior* has been observed in tunnel junctions made by means of different techniques, such as planar junctions with natural barriers,[29] point-contact junctions,[30] and vacuum tunneling spectroscopy.[31] The linearity found in these junctions could reflect a

smaller portion of the Fermi surface probed by tunneling spectroscopy, and/or to some inelastic scattering processes ocurring in the interface between the superconducting and the insulating layers.[32] The presence of this linear background can also explain the lack of conductance peaks at the gap edges. Indeed, for increasing slopes a progressive smearing of the gaplike features, together with a shift toward higher energies, has been observed. On the other hand, in the *flat behavior* conductance peaks at the gap edges are easily identified.[27] Indeed, the thickness of the barrier layer is associated with the lack of inelastic scattering processes in the interface.

In the *intermediate range* the curves reported in Fig. 5(b) show a change of slope for a sample and a conductance peak at the gap edge for another sample, indicative of a gaplike structure at about $V_g = 30-35$ mV. The gap structure has been previously determined for the Bi-based high T_C system in single crystals using native oxide barriers and metallic counterelectrodes[29] in point-contact junctions[1,33] and recently in vacuum tunneling using Au and Pt/Ir tips.[34,35] It seems that due to a slight disorder of a few coherence lengths of the top layer near the barrier, only one gap is resolved. This lowering of 2Δ, where $\Delta = eV_g/2$, may be due to the degradation of the interface which occurs during deposition of the layers.

In an ideal SIS tunnel junction the interface is defined by a very sharp transition between the superconducting and insulating region within the coherence length ξ. Therefore, the tunneling of quasiparticles that carry mainly information about the adjacent superconductors within ξ is characterized by only one certain gap value. Unlike the ideal SIS interface, an insulating barrier containing a high density of localized states is supposed to have a smeared-out transition of the gap value within ξ because, here, the localized states hybridize with the conduction states forming interface states. Due to the previous hypothesis our $G(V)$ curves could be well described assuming a BCS density of states

$$N_s = \mathrm{Re}\{(E+i\Gamma)[(E+i\Gamma)^2-\Delta^2]^{-1/2}\}, \quad (1)$$

with the large broadening parameter Γ, a phenomenological parameter introduced by Dynes *et al.*,[35] as large as the gap Δ. This explains the high smearing parameter Γ and an averaged gap voltage V_g.

The temperature evolution of $G(0)$ normalized by the value of the conductance at $V = 150$ mV for the curves of Fig. 5(b) is shown in Fig. 6(a). $G(0)$ is extracted from fitting the background conductance without considering the peak at zero bias, shown in the inset of Fig. 6(a). The value of $G(0)/G(150\,\mathrm{mV})$ starts to increase slowly and then shows two discontinuities: at 60 K a sudden increase starts to develop until T_C is reached, then it levels off at a constant value close to 1.[34] This behavior is expected for superconducting electrodes.[22]

We now turn our attention to the *low-voltage range* (voltages $|V| < 5$ mV) characterized by a zero-bias anomalies (ZBA) conductance peak, with its size depending on the voltage around zero voltage and temperature. The height of this peak increases as the temperature decreases; for a given temperature, the conductance decreases rapidly as bias departs from zero. ZBA in the tunneling conductance were already observed in metallic tunnel junctions with an oxide barrier as well as in Nb/*a*-Si/Nb tunnel junctions where it was proven using electron spin resonance measurements, that localized states in *a*-Si are responsible for this effect.[36] Recently, ZBA have been observed in a variety of measurement-tunneling junctions made of HTS, as well as conventional superconductors and semiconductor electrodes. Most of these ZBAs could be described by a theoretical

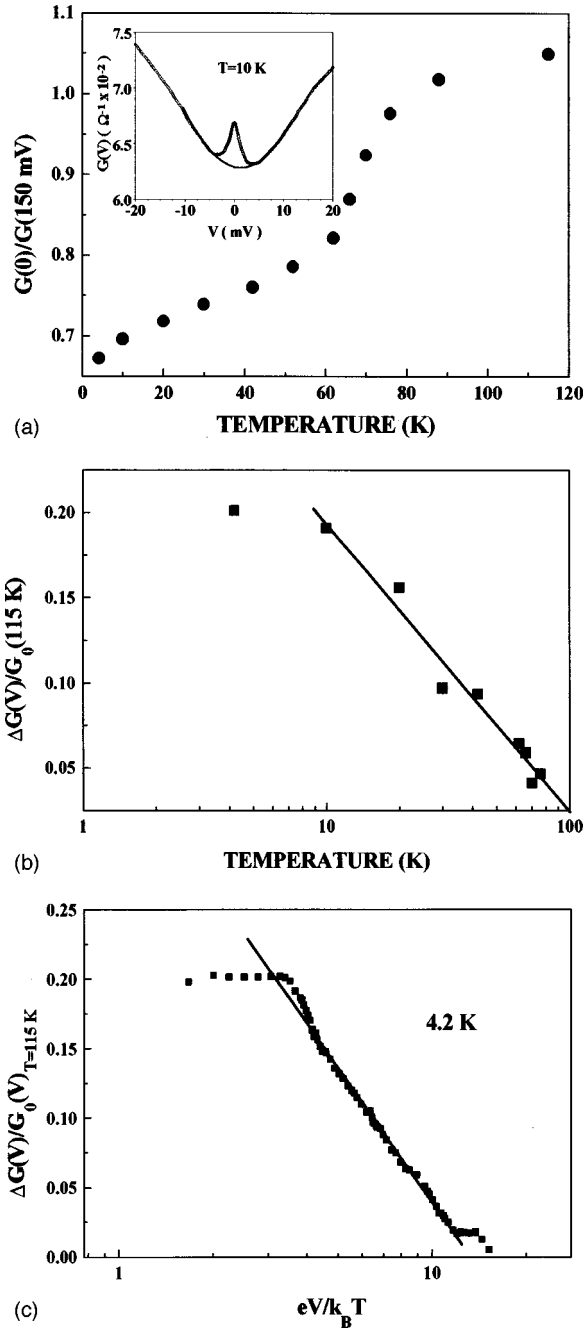

FIG. 6. (a) Normalized conductance at zero bias vs temperature; notice the two discontinuities at 60 K and around T_C. A parabolic fit (dotted line) close to zero voltage is shown in the inset, from which $G(0)$ is calculated. (b) Fractional change of the excess conductance as a function of the temperature for the sample shown in Fig. 4(b). (c) Energy dependence of the fractional change of the excess conductance for the junction shown in Fig. 4(b) at 4.2 K.

model from Appelbaum[37] and Anderson,[38] where a spin–spin interaction of the localized magnetic states with the quasiparticles opens up an additional tunnel channel increasing the conductance near zero bias. In this model a logarithmic dependence of conductance on voltage and temperature can be described by

$$\Delta G(V)=G(V,T)-G_0(V,T)=AN_1N_2\ \ln\left[\frac{E_0}{|eV|+nk_BT}\right]. \tag{2}$$

Here, A is a constant, N_1 and N_2 are the density of states of electrodes 1 and 2 in the normal state, E_0 is a cutoff energy, V is the bias voltage, T is the absolute temperature, and n is a constant of order 1. To extract the voltage and temperature dependence of ZBA, we substracted the parabolic fit to the tunneling conductance around zero bias without considering the ZBA $G_0(V,T)$ from the measured $G(V,T)$ curves, to obtain the excess conductance $\Delta G(V,T)$.

In Fig. 6(b) we show a semilogarithmic plot of the fractional change of the excess conductance as a function of the temperature for the sample of Fig. 5(b). In Fig. 6(b), the fractional change of the ZBA is 20% at 4.2 K and then decreases with increasing temperature; logarithmic behavior is evident in the range between 10 and 100 K in accordance with the Appelbaum–Anderson model, Eq. (2). The temperature T_0 at which the ZBA disappear is obtained extrapolating the line to $\Delta G(0,T)/G_0(0,T)=0$; because a normal-state property, for this junction $T_0=110$ K.

Figure 6(c) shows the energy dependence of the fractional change of the excess conductance for the junction of Fig. 5(b) at 4.2 K. Notice that at low energies the conductance drops below the linear logarithmic plot because of thermal smearing. This good agreement between measurement and theory gives strong evidence for the presence of magnetic impurities in the barrier and interface. The presence of magnetic impurities in the barrier and interface in the junctions based on HTS is explained in terms of isolated Cu magnetic moments due to possible oxygen migrations from the superconducting electrodes to the barrier, as discussed by Sanders *et al.*[39] The magnetic moments do not destroy superconductivity at the surface of the HTS electrodes, but its presence is revealed as anomalous behavior of the conductance at zero bias. Using the magnetic field from 1 to 12 T, it is possible to produce a Zeeman splitting of the impurity levels that can be attributed to the splitting of the zero-bias peak into three peaks separated by $\delta(\mathrm{mV})=g\mu_BB$ as reported by Froehlich *et al.*[40] and Sanders *et al.*[39] With our samples, the magnetic-field dependence of ΔG was not analyzed.

B. Josephson-like tunneling

For junctions with a barrier thickness of ~5 nm, a Josephson-type current at zero bias was observed. Such thickness was estimated in accordance with the deposition rate of our 22Y2 target (100 nm/h). Figure 7(a) shows typical $I-V$ curves measured for a junction with a very thin interlayer, at temperatures between 10 K and a few degrees below the transition temperature; a current at $V=0$, typical of

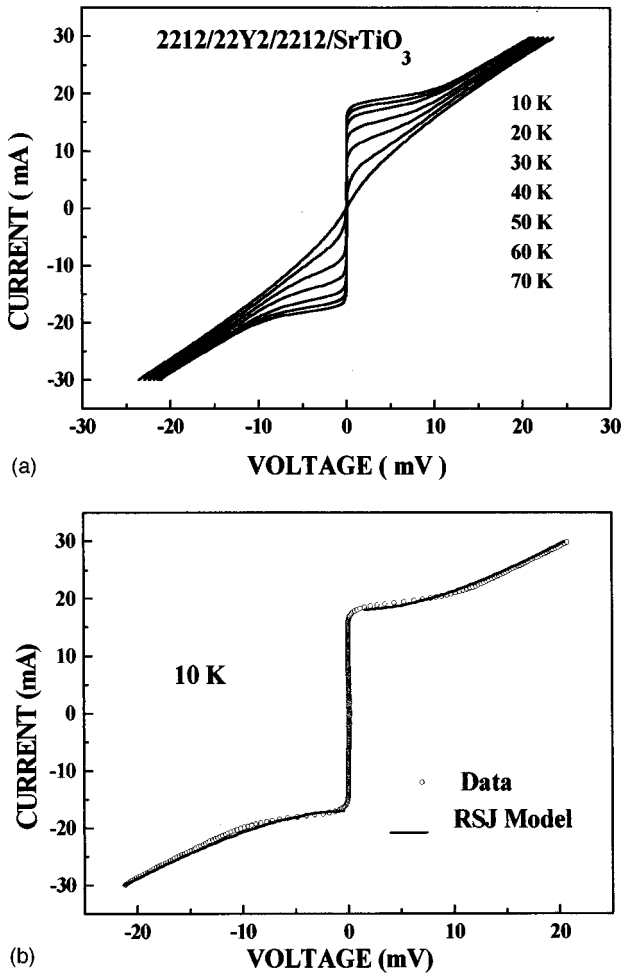

FIG. 7. (a) Current–voltage characteristics for a 2212/22Y2/2212 junction at different temperatures showing weak-link behavior. (b) RSJ model fit to the experimental I vs V at $T=10$ K.

weak-link-like behavior, is clearly apparent.[41] A small dependence of normal resistance R_n on temperature is observed as expected from the semiconducting properties of the interlayer material. The $I-V$ curves exhibit a resistively shunted junction (RSJ)[42] like behavior, as shown in Fig. 7(b). The derivation of these curves exhibits characteristic peaks which are used to obtain I_C values as a function of temperature, and normal-state resistance R_n from the slope at high voltage to obtain $V_C=I_CR_n$ values; I_CR_n product values as a function of temperature are shown in Fig. 8, where the top inset shows the $dV/dI-I$ curve at 10 K, and the bottom inset shows the critical current against reduced temperature showing a slope of 1.33 at a range near T_C. At a temperature of 10 K, typical I_CR_n products were determined to be 17 mV. The magnetic-field dependence of the critical current and/or the response of the junction to external microwave (Shapiro steps) are the best demonstration of the Josephson effect in single junctions, but these measurements were not realized. It is possibly that high critical currents and high I_CR_n-product values depend sensitively of the photolithography process used during junction preparation, which eventually leaves etch pits in the junction area. The presence of etch pits can give rise to tunneling channels along the thin barrier.

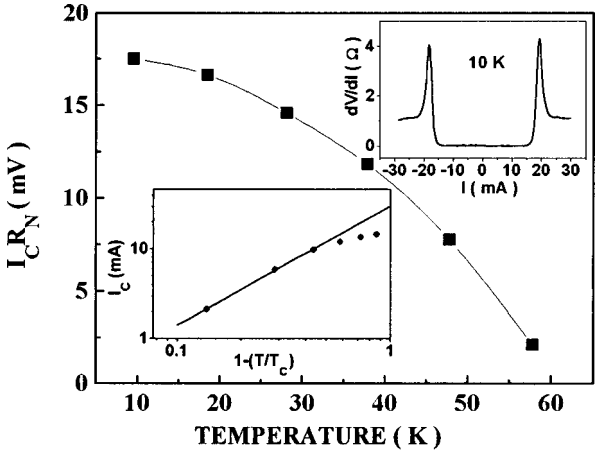

FIG. 8. Temperature behavior of the $I_C R_n$ product of a 2212/22Y2/2212 junction. Top inset illustrates the current dependence of the dV/dI, and bottom inset shows reduced temperature dependence of the critical current.

IV. CONCLUSIONS

We have fabricated high-quality 2212/22Y2/2212 trilayers on (001) $SrTiO_3$ substrates using an *in situ* dc-sputtering technique at high oxygen pressure. 22Y2 has advantages as a barrier material: its stability, the fact that it can be grown in the same deposition conditions as the 2212 layer, complete lattice matching with 2212, as well as high compatibility in composition with 2212. The conductance curves measured on 2212/22Y2/2212 junctions show quasiparticle tunneling current with a clear gaplike structure around 30 meV, a linear conductance background above the superconducting gap structure, and a ZBA which showed a strong temperature dependence understood in terms of the presence of Cu paramagnetic ions at the interface. These junctions may also show weak-link behavior if the barrier is thin enough. All of these facts make the 2212/22Y2/2212 system a potential candidate for superconducting device applications.

ACKNOWLEDGMENTS

This work was supported by COLCIENCIAS under Contracts No. 1106-05-197-95 and 361-97, by the Consiglio Nazionale delle richerche (CNR) under project ''Interface studies in high T_C based planar junctions,'' and by DGAPA-UNAM Project No. IN104793.

[1] T. Hasegawa, H. Ikuta, and K. Kitasawa, in *Physical Properties of High-T_C Superconductors III*, edited by D. M. Ginsberg (World Scientific, Singapore, 1992).
[2] J. S. Martens, D. S. Ginley, J. B. Beyer, J. E. Norman, and G. K. G. Hohenwarter, IEEE Trans. Magn. **27**, 3284 (1991).
[3] J. Z. Sun, W. J. Gallagher, A. C. Callegari, V. Foglietti, and R. Koch, Appl. Phys. Lett. **63**, 1561 (1993); see also, H. C. Yang *et al.*, J. Appl. Phys. **78**, 1871 (1995), and references therein.
[4] M. Schilling, D. Reimer, and U. Merkt, Appl. Phys. Lett. **64**, 2584 (1994); see also, Refs. 6 and 7 and references therein.
[5] C. W. Chu, IEEE Trans. Appl. Supercond. **7**, 80 (1997); see also, A. Schilling, M. Cautoni, J. D. Gao, and H. R. Ott, Nature (London) **363**, 56 (1993); L. Gao *et al.*, Phys. Rev. B **50**, 4260 (1994).
[6] I. Giaever, Phys. Rev. Lett. **5**, 147 (1960); **5**, 464 (1960).
[7] J. Moreland, J. W. Ekin, L. F. Goodrich, T. E. Capobianco, A. F. Clark, J. Kwo, M. Hong, and S. H. Liou, Phys. Rev. B **35**, 8856 (1987).
[8] Th. Becherer, J. Kowalewski, M. Schmitt, M. Huth, W. Assmus, and H. Adrian, Z. Phys. B **86**, 23 (1992).
[9] D. Mandrus, J. Hartge, C. Kendziora, L. Mihaly, and L. Forro, Europhys. Lett. **22**, 199 (1993).
[10] S. Vieira, M. A. Ramos, M. Vallet-Regi, and J. M. Gonzalez-Calbet, Phys. Rev. B **38**, 9295 (1988).
[11] T. Ekino and J. Akimitsu, Phys. Rev. B **40**, 6902 (1989).
[12] Q. Huang, J. F. Zasadzinski, K. E. Gray, J. Z. Liu, and H. Claus, Phys. Rev. B **40**, 9366 (1989).
[13] P. Chaudhari, J. Mannhart, D. Dimos, C. C. Tsuei, J. Chi, M. M. Oprysko, and M. Sheuermann, Phys. Rev. Lett. **60**, 1653 (1988); A. Kussmaul, E. S. Hellman, E. H. Hartford, Jr., and P. M. Tedrow, Appl. Phys. Lett. **63**, 2824 (1993).
[14] T. Walsh, J. Moreland, R. H. Ono, and T. S. Kalkur, Phys. Rev. Lett. **66**, 516 (1991).
[15] J. X. Liu, J.-C. Wan, A. M. Goldman, Y. C. Chang, and P. Z. Jiang, Phys. Rev. Lett. **67**, 2195 (1991).
[16] R. Laibowitz, R. P. Robertazzi, R. H. Koch, A. Kleinsasser, J. R. Kirtley, J. M. Viggiano, R. L. Sandstrom, and W. J. Gallagher, Phys. Rev. B **46**, 14 830 (1992).
[17] H. Ikuta, A. Maeda, K. Uchinokura, and S. Tanaka, Jpn. J. Appl. Phys., Part 2 **6**, L1038 (1988).
[18] H. J. Tao, A. Chang, F. Lu, and E. L. Wolf, Phys. Rev. B **45**, 10 622 (1992).
[19] A. G. Sun, D. A. Gajewski, M. B. Maple, and R. C. Dynes, Phys. Rev. Lett. **72**, 2267 (1994).
[20] See, for example, E. L. Wolf, *Principles of Electron Tunneling Spectroscopy* (Oxford University Press, New York, 1985).
[21] R. C. Dynes, Solid State Commun. **92**, 53 (1994), and references therein.
[22] A. M. Cucolo, R. Di Leo, A. Nigro, P. Romano, E. Bacca, and P. Prieto, Phys. Rev. Lett. **76**, 1920 (1996).
[23] K. Mizuno, H. Higashino, K. Setsune, and K. Wasa, Appl. Phys. Lett. **58**, 1 (1991).
[24] A. M. Cucolo, R. Di Leo, P. Romano, E. Bacca, M. E. Gomez, W. Lopera, P. Prieto, and J. Heiras, Appl. Phys. Lett. **68**, 253 (1996).
[25] C. Quitmann, D. Andrich, C. Jarchow, M. Fleuster, B. Beschoten, G. Güntherodt, V. V. Moshchalkov, G. Mante, and R. Manzke, Phys. Rev. B **46**, 11 813 (1992).
[26] E. Baca, M. Carotenuto, R. Di Leo, G. Iannone, A. Nigro, P. Romano, and A. M. Cucolo, Nuovo Cimento **16 D**, 1695 (1994).
[27] A. M. Cucolo, R. Di Leo, A. Nigro, P. Romano, E. Bacca, W. Lopera, M. E. Gomez, and P. Prieto, IEEE Trans. Appl. Supercond. **7**, 2848 (1997).
[28] N. F. Mott and E. A. Davis, *Electronic Processes in Non-Crystalline Materials*, 2nd ed. (Claredon, Oxford, 1979), Chaps. 1 and 6.
[29] A. M. Cucolo, R. Di Leo, A. Nigro, P. Romano, and M. Carotenuto, Phys. Rev. B **49**, 1308 (1994).
[30] J. F. Zasadzinnski, N. Tralshawala, P. Romano, Q. Huang, J. Chen, and K. E. Gray, J. Phys. Chem. Solids **53**, 1635 (1992).
[31] Ch. Renner and O. Fischer, Phys. Rev. B **51**, 9208 (1995).
[32] J. R. Kirtley and D. J. Scalapino, Phys. Rev. Lett. **65**, 798 (1990).
[33] H. J. Tao, A. Chang, F. Lu, and E. L. Wolf, Phys. Rev. B **45**, 10 622 (1992).
[34] E. Bacca, M. E. Gómez, J. Heiras y P. Prieto, A. M. Cucolo, R. Di Leo, P. Romano, and y A. Nigro, Solid State Commun. **102**, 425 (1997).
[35] R. C. Dynes, V. Narayanamurti, and J. P. Garno, Phys. Rev. Lett. **41**, 1509 (1987).
[36] A. F. G. Wyatt, Phys. Rev. Lett. **13**, 401 (1964).
[37] J. Appelbaum, Phys. Rev. Lett. **17**, 91 (1966).
[38] P. W. Anderson, Phys. Rev. Lett. **17**, 95 (1966).
[39] S. C. Sanders, S. E. Russek, C. C. Clickner, and J. W. Ekin, IEEE Trans. Appl. Supercond. **5**, 2404 (1995).
[40] O. M. Froehlich, P. Richter, A. Beck, D. Koelle, and R. Gross, IEEE Trans. Appl. Supercond. **7**, 3189 (1997).
[41] E. Bacca, M. Chacón, L. F. Castro, M. E. Gómez, and P. Prieto, Physica C **235–240**, 727 (1994).
[42] V. Ambegeokar and A. Baratoff, Phys. Rev. Lett. **10**, 486 (1963).